Adiabatic and Non-Adiabatic Resonances in Excitable Systems

André Longtin

Département de Physique, Université d'Ottawa
150 Louis Pasteur, Ottawa, Ontario, Canada K1N 6N5

Abstract. This paper discusses recent developments in the study of resonances in stochastic excitable systems. It describes how the classical phase locking regions in the forcing amplitude-forcing period subspace are modified by noise, and how an extension of this subspace that includes noise intensity reveals new features of stochastic phase locking and stochastic resonances. It also briefly reviews neuron models used to investigate these issues, and in particular contrasts their coupling of noise to the excitable dynamics.

1 Introduction

The response of excitable systems to deterministic and/or stochastic forcing has received much attention in the last decades (Glass and Mackey, 1988). Responses to suprathreshold periodic forcing include n:m phase locking patterns with m firings for n forcing cycles, as well as chaotic firing patterns. These patterns result from the nonlinear interaction of internal time scales with the external time scale of the input. Stochastic forcing further turns a quiescent excitable system into a stochastic oscillator (Treutlein and Schulten 1985). This can modify the phase locking structure, and can strongly affect the frequency sensitivity ("tuning") characteristics of the cells (Collins et al, 1995; Longtin 2000). Furthermore, other new phenomena arise from stochastic forcing, such as coherence resonance (Pikovsky and Kurths 1977), stochastic resonance (Gammaitoni et al. 1998), mean frequency locking (Shulgin et al., 1995) and noise-enhanced phase coherence (Neiman et al., 1998). At the core of these phenomena lies the concept of resonance.

Our paper is a brief survey of deterministic and stochastic resonances in neural systems with periodic and/or stochastic forcing. It is not meant to be comprehensive. Rather, its intent is to summarize and contrast some of the major models recently used to study these phenomena, and to present recent developments in the study of such resonances. We are primarily concerned with the effects of neural noise, due e.g. to ionic channel conductance, synaptic failure, and random synaptic inputs, rather than of random physical stimuli. Section 2 describes three popular neuron models used to study stochastic neural dynamics. Section 3 looks at a neural input-output function and at how neural noise can linearize this function. Section 4 discusses deterministic resonance, and how noise turns the excitable system into a stochastic oscillator and associated consequences for tuning. Section 5 considers a new representation of phase locking patterns in parameter space, and discusses multiple stochastic resonances. Perspectives on suprathreshold noisy phase locking for modeling purposes are the subject of Sect.6, and the paper concludes in Sect.7.

2 Basic Neuron Models

The standard dynamical description of a neuron is in terms of the Hodgkin-Huxley formalism:

$$\begin{aligned} CdV/dt &= \sum I_{ion} + I_{syn} + I_{app} \qquad (1)\\ &= \sum_i g_i s_i S_i (V_i - V) + g_{exc}(V_{exc} - V) + g_{inh}(V_{inh} - V) + I_{app} \end{aligned}$$

where V is the voltage at the spike generating zone, and C the membrane capacitance. I_{app} designates external bias currents. I_{ion} accounts for the non-synaptic ionic currents. Synaptic currents are divided into excitatory currents, $g_{exc}(V_{exc} - V)$, and inhibitory currents, $g_{inh}(V_{inh} - V)$. The V_i are the Nernst "reversal" potentials for each ionic species, and V_{exc} and V_{inh} are, respectively, the excitatory and inhibitory reversal potentials for each particular synapse. The g_i's are the maximal conductances, and s_i and S_i are, respectively, activation and inactivation gating variables. The latter, which take on values between zero and one, follow first-order dynamics with voltage-dependent parameters. The excitatory (g_{exc}) and inhibitory (g_{inh}) synaptic conductances may also involve gating variables.

The effect of synaptic input at a given time depends on the value of the voltage. For example, if the voltage is equal to the reversal potential for a given synapse, any amount of synaptic conductance change will nevertheless produce zero current from that synapse. Under certain conditions, such as when conductance changes are small compared to the inverse of the input resistance of the cell membrane, and when the reversal potential exceeds the threshold voltage, synaptic input can be approximated as a constant current source $I_{syn} = V_{syn} g_{syn}$ (see e.g. Koch 1999). This is often assumed in simple integrate-and-fire type models (see below, and e.g. Brunel and Sergi, 1998). Further, the arrival of action potentials at synapses can be modeled as a train of Dirac delta functions, such that if the voltage dependence is neglected, $I_{syn}(t) = \sum_i^N \sum_j J_i \delta(t - t_i^j)$, where the first sum is over all N synapses, and the second, over all firing times t_i^j at each synapse; J_i is the synaptic efficacy, related to its maximal conductance.

An input spike train is often assumed to be a Poisson process with rate $N\nu$, where ν is the mean rate at each synapse. If ν is small, and the J_i are small (i.e. many synaptic events are needed to fire the cell), yet $N\nu \gg 1$, the Poisson process can be approximated by a diffusion process with same mean and variance. For the simple case $J_i = J$, we have the mean $\mu = J\nu N$, and the correlation function is $\langle I_{syn}(t) I_{syn}(t')\rangle = \sigma^2\delta(t-t') = J^2\nu N\delta(t-t')$, where σ denotes the intensity of this white noise process. In this case, and assuming the voltage-independent approximation discussed above, synaptic input may be modeled as Gaussian white additive noise on the voltage dynamics. Further, synapses also have their own (usually) first-order dynamics. Then, if the diffusion approximation is valid, the first-order synaptic current dynamics are approximately driven by Gaussian white noise (see e.g. Brunel and Sergi, 1998); in other words, the synaptic current is a lowpass-filtered version of the train of delta-functions. $I_{syn}(t)$ is then an Ornstein-Uhlenbeck (OU) process, which in turn drives the voltage dynamics at the spike generating zone of the neuron. This justifies using OU noise for input to other models such as the analytically and computationally simpler Fitzhugh-Nagumo (FHN) model. This reduced model is obtained from HH by keeping only the fast voltage variable v and a slow recovery variable w. Below we focus on this model with additive periodic and/or stochastic forcing (Longtin 1993):

$$\epsilon\frac{dv}{dt} = v(v-0.5)(1-v) - w + A\sin\omega_0 t + I + \eta(t) \tag{2}$$

$$\frac{dw}{dt} = v - w - b\,. \tag{3}$$

The bias current I encompasses the mean external and synaptic currents, and η is an Ornstein-Uhlenbeck (OU) noise with correlation time t_c and variance D/t_c; for the simulations presented below, D will denote the noise intensity of this OU process. This noise is useful to investigate the effect on the dynamics of noise variance and bandwidth. Below, this system was integrated as in Longtin and Chialvo (1998). FHN still has realistic excitable dynamics with a deterministic resonance as many neurons do (Guttman et al.1974). Our parameters are $I = 0.04, b = 0.15, \epsilon = 0.005$, $t_c = 10^{-3}$, the threshold is 0.5, and a firing is counted only if separated from a previous one by at least the refractory time of $T_R = 0.4$ sec (equivalent to $\approx 1-2$ msec in real time).

A leaky integrate-and-fire one-dimensional model (LIF) (Knight, 1972) assumes that the g_i in HH are not voltage-dependent (gating variables are zero or one):

$$C\frac{dV}{dt} = g_L(V_L - V) + g_{exc}(V_{exc} - V) + \tag{4}$$

$$= g_{inh}(V_{inh} - V) + \sum_{g_i} g_i(V_i - V) + I_{app} \tag{5}$$

The voltage is reset to H after the voltage reaches a threshold value θ. Synaptic inputs simply modify g_{exc} and g_{inh} in time, and as mentioned above, in the simplest cases, synaptic current does not depend on V but simply enters the dynamics additively.

3 Linearization of the Transfer Function

An excitable system can be described by a transfer function or "transduction" function, i.e. a function that relates the instantaneous firing rate to the instantaneous value of the input current (usually synaptic or from an external current source). Sufficiently slow signals can then be seen as modulating the input currents, and via the transduction function, the firing rate. Furthermore, this function depends on the intensities of the stochastic processes driving the neuron. We begin by quoting a result due to Ricciardi (1977) for the mean firing rate R of a LIF neuron governed by the dynamical equation:

$$C\frac{dV}{dt} = -gV + I + \sigma\xi(t)\,, \tag{6}$$

where g is assumed here to be a constant, I a constant bias current, and $\sigma\xi(t)$ is the stochastic input current of intensity σ. This rate is given by:

$$R = \left(\tau_{ref} + \sqrt{\pi}\tilde{\tau}_m \int_{\frac{C(H-V_{ss})}{\sigma\sqrt{\tau}}}^{\frac{C(\theta-V_{ss})}{\sigma\sqrt{\tau}}} dx\, \exp(x^2)\,[1 + erf(x)]\right)^{-1} . \tag{7}$$

Here τ_{ref} is the absolute refractory period, $\tilde{\tau}_m = C/g$ is the membrane time constant, θ is the threshold voltage, H is the reset voltage after a spike, and V_{ss} is the steady state voltage for $\sigma = 0$: $V_s s = I/g$. A plot of $R(I)$ versus I yields a sigmoidal function (Fig.1a). Since R is also a monotonically increasing function of σ, the sigmoid for σ_1 lies under that for $\sigma_2 > \sigma_1$. We show here that the quantity $\partial R/\partial I$ gives the behavior of the slope of this transfer function as a function of σ. This slope is given by

$$\frac{\partial R}{\partial I} = -\frac{R^2}{\sigma} \exp\left(\frac{\theta - I}{\sigma}\right)\left[1 + \text{erf}\left(\frac{\theta - I}{\sigma}\right)\right]$$
$$+\sigma^{-1} \exp\left(\frac{H - I}{\sigma}\right)\left[1 + \text{erf}\left(\frac{H - I}{\sigma}\right)\right] \tag{8}$$

A plot of this slope versus σ is given in Fig.1b. The non-monotonicity of this relation accounts for the low-frequency SR exhibited by this model (Bulsara et al., 1996; Shimokawa et al., 1999a, 1999b). This is because a slow input signal is equivalent to a slow variation of the current I. In turn, slow variations of I are translated into slow variations of the firing rate. The linearity of this relationship is maximized at an intermediate value of σ. A plot of the mean firing rate versus the bias parameter also yields a sigmoidal function for the stochastic FHN system (Treutlein and Schulten, 1985; Collins et al, 1995; Chialvo et al, 1997). The dependency of this slope on noise intensity also underlies, for slow signals, the non-monotonicity versus noise intensity of quantities such as the power spectral amplification or the linear correlation between the input signal and the firing rate averaged over a small time window. The value of noise intensity that maximizes such quantities is found to be independent of the frequency of the signal in this slow signal limit (Longtin and Chialvo, 1998; see also Jung 1994).

4 Deterministic Resonance and Spontaneous Firing

The models described above have an autonomous oscillation regime arising via a bifurcation from an excitatory regime as e.g. I_{app} is increased. The HH and FHN models have a deterministic resonance; they behave as underdamped oscillators. The LIF model above does not. Figure 2 shows the organization of different steady-state periodic firing patterns in the usual signal amplitude-period subspace for the FHN model described in Sect.2. Only three are shown for $D = 0$. The curves correspond to A,T pairs above which a given *n:m* locking occurs (Arnold tongue boundaries). The subthreshold regime lies below the 1:0 curve. One sees that the threshold for a given n:m firing depends on $T = 2\pi/\beta$, and is lowest for a "preferred period". The preferred period for 1:1 is close to the period of the limit cycle that is reached for larger I_{app}, and to the value of T yielding the largest subthreshold voltage response.

In the presence of noise and without signal, "spontaneous firing" occurs. Because of the resonant nature of the FHN and HH systems, this noisy firing has a certain coherence (Longtin 1993). In fact, this coherence can be maximized by a finite noise intensity (Pikovsky and Kurths, 1997; Lindner and Schimansky-Geier, 1999). In other words, the noise induces the limit cycle from the excitable regime, a phenomenon referred to in this context as coherence resonance.

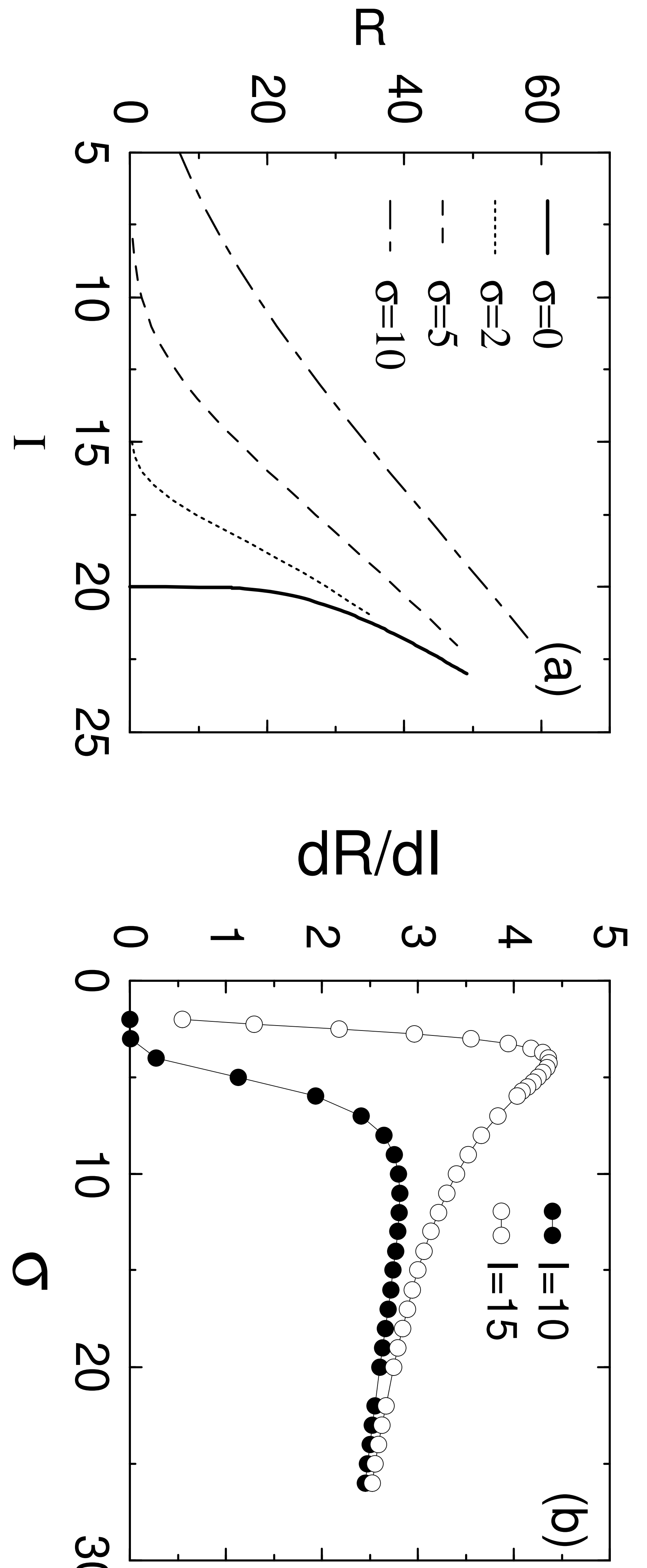

Fig. 1. a) Mean firing rate (in Hz) of a leaky integrate and fire model as a function of mean bias current I according to Eq.7 with $\tau_{ref} = 2msec$, $\tau_m = 10$ msec, $H = 0$ and $\theta = 20$ (as in Brunel, 1996). Note that the maximal firing rate is $1/\tau_{ref} = 500$ Hz. b) The slope dR/dI calculated from Eq.8 versus the intensity σ of the stochastic input current.

With periodic forcing, the 1:0 boundary no longer exists, and the noise blurs the boundaries between the phase locking curves. Each curve can now be interpreted as the set of A-T parameter pairs yielding a given time-averaged phase locking ratio (see e.g. Longtin, 2000). Thus, an $n:1$ ratio means an *aperiodic firing pattern* with one spike for n stimulus cycles on average. Figure 2 shows that the noise opens up the Arnold tongues at periods larger than the preferred period. Our recent study (Longtin 2000) has shown that the shape of these tuning curves for $T > 1.5$ can be deduced from an adiabatic theory based on an Arrhenius law. However, the frequency dependence of the subthreshold voltage response, related to the deterministic resonance, must be taken into account. Without this, two forcings with same A but different T would be expected to produce the same mean firing rate, which is clearly not the case (Fig.2). Forcing near the preferred T produces the largest voltage excursions, increasing the likelihood of firings. For $T < 1.5$, the recovery variable also determines the firing probability, and the escape time problem is then intrinsically two-dimensional.

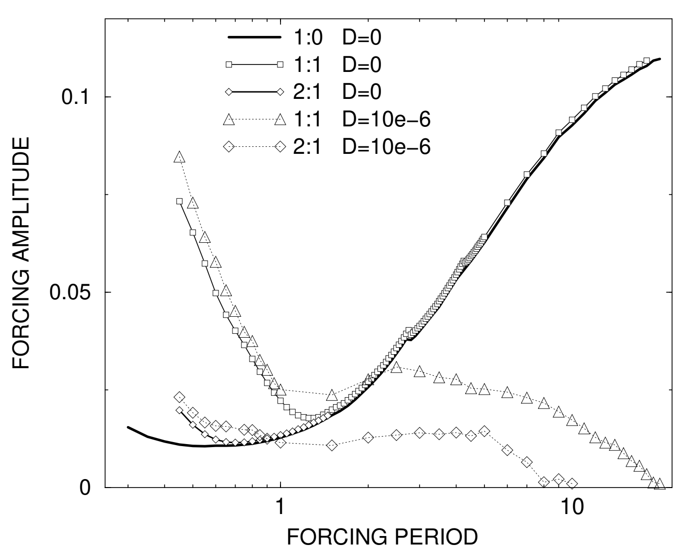

Fig. 2. Boundaries between phase locking patterns in the standard forcing amplitude-forcing period subspace for Eqs.3. The $1:0$, $D = 0$ curve defines the boundary between sub- and suprathreshold amplitudes. The V-shape of the $D = 0$ boundaries is due here to the use of sinusoidal forcing. For finite D, the average curves $\langle 1:1 \rangle$ and $\langle 2:1 \rangle$ move into the "subthreshold" region for $T > 1.3$.

5 $D-T$ Subspace and Stochastic Resonance

We now consider the noise intensity-forcing period "$D-T$" subspace for the study of stochastic phase locking and resonances. Figure 3 shows the location of the 1:1 "DT" stochastic phase locking curves for three values of A. The curves are either monotonic or non-monotonic. For $A = 0.01$, the forcing is always subthreshold, and a monotonic curve results. For $A = 0.015$, the forcing is actually suprathreshold over a certain range of T, but the curve is nevertheless monotonic. Higher amplitudes can be seen as bringing on resonances (there are actually two dips for $A = 0.02$) from this DT perspective. And for certain $A-T$ combinations, the system is already firing in a 1:1 manner without noise, as is the case for $A = 0.03$ for $1 < T < 2$. We also note a recent study of higher (but subthreshold) amplitude SR in a LIF model (Shimokawa et al., 1999b) in which mean discharge frequency locking was found to underlie signal enhancement. At higher frequencies, nonlinear phase

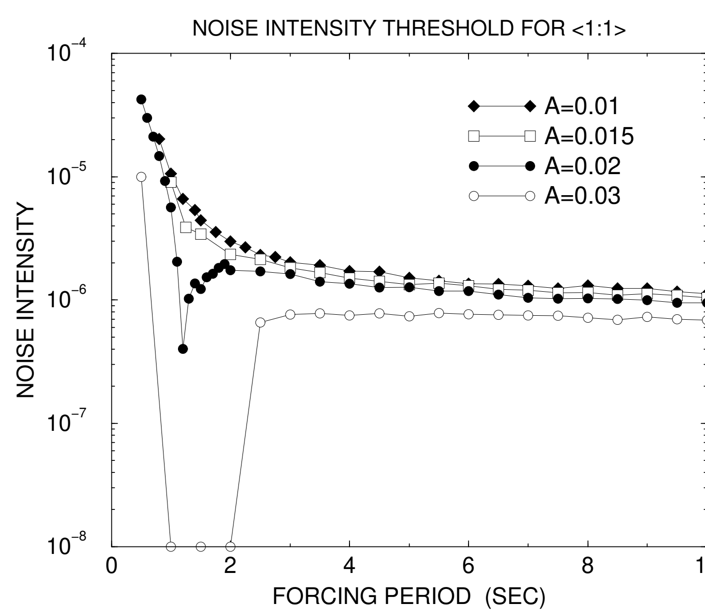

Fig. 3. Stochastic phase locking curves in the D-T subspace for different sinusoidal forcing amplitudes A in the FHN system. Points correspond to averages over three realizations of 100 periods. For $A = 0.02$, the forcing is suprathreshold for $T < 1.7$, and for $T < 1.21$ for $A = 0.015$. Also, for $A = 0.03$, the points on the x-axis actually correspond to $D = 0$.

locking phenomena occur in the suprathreshold regime (see also Shulgin et al. 1995). For subthreshold signals, multiple stochastic resonances can occur as D increases (Longtin and Chialvo, 1998). Here we report on a transition for a single to a double stochastic resonance as D increases. Figure 4 shows the power spectral density at the driving frequency for increasing D. For $T = 1.1$, a single maximum is seen, while for $T = 0.6$, two bumps are seen. Such multiple resonances were found when $T < 0.9$. Similar resonances have also been found in bistable systems (Jung and Hanggi, 1991). These subthreshold resonances are perhaps related to the deterministic lockings that exist for suprathreshold forcing, and which are induced by the noise. This is currently under investigation.

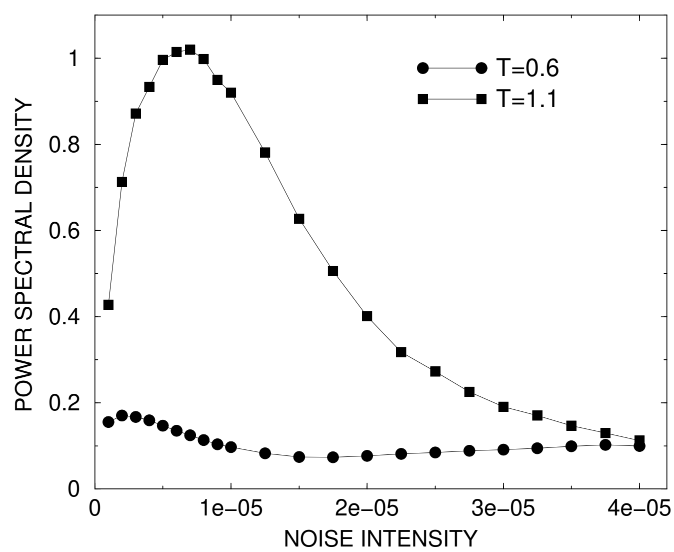

Fig. 4. Power spectral density (PSD) at the forcing frequency $S(\omega_o)$ computed versus D from spike trains for the FHN system. For each combination of period and noise intensity, the PSD was calculated from 50 realizations of 340 periods of the stimulus.

6 Skipping from Suprathreshold Regime

There has been much focus in the SR literature on the stochastic phase locking that occurs when a subthreshold periodic signal drives a noisy nonlinear system. This produces the familiar multimodal residence time histograms (Gammaitoni et al., 1998). Suprathreshold signals can also produce such behavior in the FHN system (Longtin, 1993). However, the histogram peaks in that study did not properly align with the integer multiples of the forcing period, and the histogram envelope did not vary smoothly with forcing paramaters as it did in experimental data and in the subthreshold regime. This was in part ascribed to the blurring of chaotic motion by noise.

In Fig.5 we show new results from a simulation of the FHN system at higher frequencies than those used in our previous study. The value of I is also higher (0.04 instead of 0.0), b is 0.15 rather than 0.2, and the forcing here is applied directly to the fast variable rather than the slow one as was done in Longtin 1993. The left panel shows the interspike interval histogram for the noiseless dynamics; the motion is a 5:1 phase locking. Additive noise here causes the histogram to become multimodal with well-aligned peaks and smooth envelope variations. There does not seem to be much chaotic activity nearby in parameter space. Also, the sinusoidal signal here is now actually rectified, i.e. only its positive part drives the voltage dynamics; the results are qualitatively similar even without rectification. Such rectification is justified for many sensory neurons which respond to only one polarity of a physical stimulus (such as the opening of channels when hair cells are bent in one direction). P-type electroreceptors of weakly electric fish exhibit histograms such as those in Fig.5b. Our recent study, based on a two-dimensional version of an LIF model to account for firing interval correlations, supports the notion of suprathreshold noisy dynamics in those cells (Chacron et al, 2000). This motivates further theoretical studies of escape time distributions for suprathreshold dynamics.

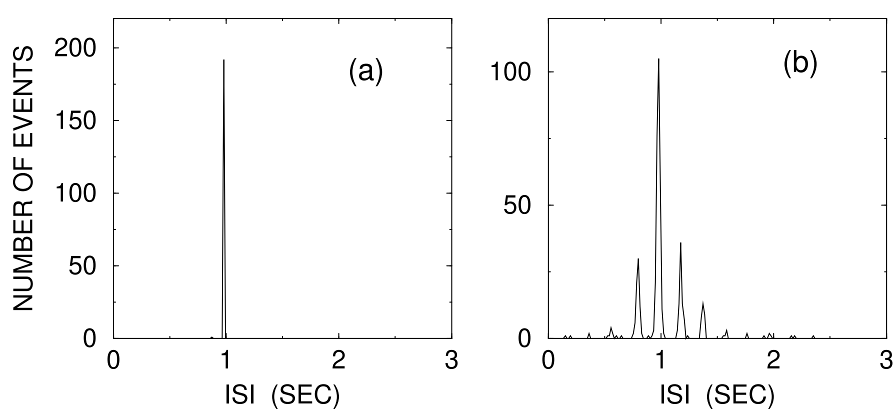

Fig. 5. Smooth skipping-type firing patterns in the higher frequency suprathreshold regime of the FHN system. Interspike interval histograms are for (a) $D = 0$ (5 : 1 phase locking and (b) $D = 4 \times 10^{-6}$. Parameters are $\omega_o = 32$, $A = 0.06$ and a rectified sinusoidal forcing is used to mimick synaptic input.

7 Conclusion

We have shown that the addition of noise to excitable dynamics brings a new perspective on issues of resonance and tuning. Noise linearizes the transduction function of the neuron, allowing its firing rate to track slow input signals.

It also changes the shape of tuning curves, especially for forcing frequencies below the preferred frequency of the neuron, i.e. toward the adiabatic regime. For higher frequencies, i.e. in the non-adiabatic regime of the neuron (Longtin and Chialvo, 1998; Massanes and Perez Vicente, 1999 ;see also Plesser and Geisel, 1999 for the LIF case), subthreshold resonances appear in the behavior of certain firing statistics; in fact, many can appear, as though statistical versions of the deterministic phase locking boundaries are expressed by noise in the subthreshold regime. The study of those resonances will likely require analyses of the dynamics that account for the recovery variable behavior, such as the one recently proposed by Lindner and Schimansky-Geier (2000). This is likely to be the case as well for the study of the supra-and subthreshold resonances found in the DT subspace (Fig.3).
This research was supported by NSERC (Canada). We thank Adi Bulsara, Jan Freund, Lutz Schimansky-Geier, Khashayar Pakdaman and Dante Chialvo for useful discussions in relation to this work.

References

1. Brunel, B. (1996) Neural Comput. **8**, 1677.
2. Brunel, N. and Sergi, S. (1998) J. theor. Biol. **195**, 87.
3. Bulsara, A.R. *et al.* (1996) Phys. Rev. E **53**, 3958.
4. Chacron, M., Longtin, A., St-Hilaire, M. and Maler, L. (submitted).
5. Chialvo, D.R., Longtin, A. and Müller-Gerking, J. (1997) Phys. Rev. E **55**, 1798.
6. Collins, J.J., Chow, C.C. and Imhoff, T. (1995) Phys. Rev. E **52**, R3321.
7. Gammaitoni, L., et al. (1998) Rev. Mod. Phys. **70**, 223.
8. Glass L. and Mackey, M.C. (1988) From Clocks to Chaos. The Rhythms of Life. Princeton University Press, Princeton, N.J.
9. Guttman, R., Feldman, L. and Lecar, H. (1974) Biophys. J. **14**, 941.
10. Jung, P. (1994) Phys. Rev. E **50**, 2513.
11. Jung, P. and Hänggi, P. (1991) Phys. Rev. A **44**, 8032.
12. Knight, B.W. (1972) J. gen. Physiol. **59**, 734.
13. Koch, C. (1999) Biophysics of Computation (Oxford University Press, New York).
14. Lindner, B. and Schimansky-Geier, L. (2000) Phys.Rev. E **60**, 7270.
15. Lindner, B. and Schimansky-Geier, L. (2000) Phys.Rev. E (in press).
16. Longtin, A. and Chialvo, D. (1998) Phys. Rev. Lett. **81**, 4012.
17. Longtin, A. (1993) J. Stat. Phys. **70**, 309.
18. Longtin, A. (2000) Chaos Solit. Fract. (in press).
19. Massanes, S.R. and Perez Vicente, C.J. (1999) Phys. Rev. E **59**, 4490.
20. Neiman, A. et al. (1998) Phys. Rev. E **58**, 7118.
21. Pikovsky, A. and Kurths, J. (1997) Phys. Rev. Lett. **78**, 775.
22. Plesser, H.E. and Geisel, T. (1999) Phys. Rev. E **59**, 7008.
23. Ricciardi, L.M. (1977) Diffusion Processes and Related Topics on Biology. Berlin, Springer-Verlag.
24. Shimokawa, T., Pakdaman, K. and Sato, S. (1999a) Phys. Rev. E **59**, 3427.
25. Shimokawa, T., Pakdaman, K. and Sato, S. (1999b) Phys. Rev. E **60**, R33.
26. Shulgin, B. *et al.* (1995) Phys. Rev. Lett. **75**, 4157.
27. Treutlein, H. and Schulten, K. (1985) Ber. Bunsenges. Phys. Chem. **89**, 710.